analytical chemistry

Article

Exploring the Potential of Stable Isotope (Resonance) Raman Microspectroscopy and SERS for the Analysis of Microorganisms at Single Cell Level

Patrick Kubryk, Janina S. Kölschbach, Sviatlana Marozava, Tillmann Lueders, Rainer Udo Meckenstock, Reinhard Niessner, and Natalia P. Ivleva

Anal. Chem., **Just Accepted Manuscript** • DOI: 10.1021/acs.analchem.5b00673 • Publication Date (Web): 26 May 2015

ACS Publications
High quality. High impact.

Analytical Chemistry is published by the American Chemical Society. 1155 Sixteenth Street N.W., Washington, DC 20036

Exploring the Potential of Stable Isotope (Resonance) Raman Microspectroscopy and SERS for the Analysis of Microorganisms at Single Cell Level

Patrick Kubryk[1], Janina S. Kölschbach[2], Sviatlana Marozava[2], Tillmann Lueders[2], Rainer U. Meckenstock[2, 3], Reinhard Niessner[1], Natalia P. Ivleva[1, *]

[1]Technische Universität München, Institute of Hydrochemistry, Chair for Analytical Chemistry, Marchioninistr. 17, 81377 Munich, Germany

[2]Helmholtz Zentrum München, Institute of Groundwater Ecology, Ingolstädter Landstr. 1, 85764 Neuherberg, Germany

[3]present address: University of Duisburg-Essen, Biofilm Centre, Chair for Aquatic Microbiology, Universitätsstr. 5, 45141 Essen, Germany

*Corresponding author: Tel.: +49 2180 78238; Fax: +49 2180 78255; E-mail: natalia.ivleva@ch.tum.de

Abstract

Raman microspectroscopy is a prime tool to characterize the molecular and isotopic composition of microbial cells. However, low sensitivity and long acquisition times limit a broad applicability of the method in environmental analysis. In this study, we explore the potential, the applicability and the limitations of stable isotope Raman microspectroscopy (SIRM), resonance SIRM, and SIRM in combination with surface-enhanced Raman scattering (SERS) for the characterization of single bacterial cells. The latter two techniques have the potential to significantly increase sensitivity and decrease measurement times in SIRM, but to date there are no (SERS-SIRM) or only a limited number (resonance SIRM) of studies in environmental microbiology. The analyzed microorganisms were grown with substrates fully labeled with the stable isotopes ^{13}C or ^{2}H and compounds with natural abundance of atomic isotopes (^{12}C 98.89% or ^{1}H 99.9844%, designated as ^{12}C- or ^{1}H-, respectively). Raman bands of bacterial cell compounds in stable isotope-labeled microorganisms exhibited a characteristic red-shift in the spectra. In particular the sharp phenylalanine band was found to be an applicable marker band for SIRM analysis of the *Deltaproteobacterium* strain N47 growing anaerobically on ^{13}C-naphthalene. The study of *G.*

metallireducens grown with ^{13}C- and ^{2}H-acetate showed that the information on the chromophore cytochrome *c* obtained by resonance SIRM at 532 nm excitation wavelength can be successfully complemented by whole-organism fingerprints of bacteria cells achieved by regular SIRM after photobleaching. Furthermore, we present here for the first time the reproducible SERS analysis of microbial cells labeled with stable isotopes. *Escherichia coli* strain DSM 1116 cultivated with ^{12}C- or ^{13}C-glucose was used as a model organism. Silver nanoparticles synthesized *in situ* were applied as SERS media. We observed a reproducible red-shift of an adenine-related marker band from 733 cm^{-1} to 720 cm^{-1} in SERS spectra for ^{13}C-labbeled cells. Additionally, Raman measurements of $^{12}C/^{13}C$-glucose and –phenylalanine mixtures were performed to elucidate the feasibility of SIRM for nondestructive quantitative and spatially-resolved analysis. The performed analysis of isotopically labeled microbial cells with SERS-SIRM and resonance SIRM paves the way towards novel approaches to apply Raman microspectroscopy in environmental process studies.

Keywords

Stable Isotope Raman Microspectroscopy (SIRM), Resonance SIRM, Surface-Enhanced Raman Scattering (SERS), Bacteria, Single Cells

Introduction

Raman microspectroscopy is a combination of Raman spectroscopy and confocal microscopy. It is nondestructive / noninvasive and has a spatial resolution of down to 1 µm. The technique can provide information on molecular structures in single cells without the interference of water. Single cell Raman microspectroscopy is often used to differentiate between microbial species or to monitor the physiological state of a cell. To this end, "whole-organism fingerprints" of single cells are generated and compared to each other.[1,2]

Due to the low quantum efficiency of the Raman effect (typically $10^{-6} – 10^{-8}$), Raman spectroscopy has only a limited sensitivity. This usually leads to long acquisition times, especially for the analysis of single cells with very little biomass. However, Raman signals can be enhanced by attached, nanometer-sized metallic structures (Ag or Au). This enhancement effect is known as surface-enhanced Raman scattering (SERS). Enhancement factors of the Raman signal in the range of $10^3 – 10^{11}$ can be achieved due to electromagnetic ("localized surface plasmon resonance") and chemical ("charge transfer") enhancement effects.[3,4] By improving the Raman sensitivity with SERS, a rapid analysis and identification of single cells becomes possible.[5-7] However, SERS also comes with some limitations. First, not all Raman bands are enhanced to the same extent. For example, it is known that the enhancement of the phenylalanine band is quite low or even nonexistent in SERS spectra of bacteria.[8] Second, assuming that the production of the silver nanoparticles (AgNP) is reproducible, there are other factors such as the cultivation of the bacteria itself which can cause problems in the reproducibility of the SERS signals. Furthermore, there is usually no specific and only poor attachment of the silver colloids to bacterial cell walls causing a high heterogeneity of the SERS spectra. One method to overcome inefficient attachment of the silver nanoparticles is by increasing the concentration of the silver colloidal solution.[9] Unfortunately this hinders a controlled agglomeration of AgNP on the cell wall. As a result the signals of different cell constituents are enhanced, which also causes a high heterogeneity in the spectra. Thus, as stated by Wang et al.[10], a reproducible SERS measurement on single cells has not yet been demonstrated to date and only averaged SERS spectra would account for all the variances and would enable a comparison between different samples.[11] However, this would contradict the approach of analyzing and comparing single cells. Nevertheless, we recently reported a highly sensitive SERS detection of *E. coli* bacteria in water using *in situ* prepared AgNP.[12] Thus, a similar but slightly modified approach was chosen here to combine, for the first time, the approaches of SIRM and SERS.

Besides SERS there are other strategies to amplify the Raman signal and shorten the acquisition time. One of them is resonance Raman scattering. The resonance Raman effect occurs when the incident wavelength lies within or is close to an electronic transition of a molecule. When the microbial sample possesses resonance Raman active substances, e.g. chromophores such as heme[13], vitamin B12[14], chlorophyll[15], cytochrome *c*[16], carotenoids[17], rhodopsin[18] or flavin nucleotides[19], a more rapid Raman analysis is simply possible by choosing an appropriate laser wavelength (mostly green).[20] Measurement times of down to 1 ms for bacterial cells thus become possible.[21] If none of these substances are present or usable, an ultraviolet laser can be chosen where aromatic amino acids and nucleic acids are in resonance.[22,23]

All three techniques, Raman microspectroscopy, SERS, and resonance Raman microspectroscopy, have the potential to detect stable isotope labeling of cells. When an atom is substituted by a(n) (stable) isotope of the same element, the change of the chemical structure of the molecule is negligible and the intensity of corresponding vibration bands remains the same. However, the vibrational frequency of the involved bond(s) is affected significantly. In the case of heavier isotopes such as ^{13}C, the corresponding Raman band is red-shifted in the spectrum. The exact value of the red-shift is dependent on the exact mass change. More precisely, the red-shift is inversely proportional to the square root of the atomic mass.[1,20] Stable isotope Raman microspectroscopy (SIRM) has a big potential for analysis of isotope tracer incorporation into biomass.[24] It has been applied to diverse fields of microbiology research, and has revealed the extracellular activity of chlamydiae[25], carbon dioxide fixation by single cells[21], carbon flow in a microbial food chain[26] and active metabolic pathways in yeast[27]. It was observed by Li et al.[26] that *E. coli* cells grown with different mixtures of ^{12}C/^{13}C-glucose showed a linear correlation of the ratio of the ^{13}C over ^{12}C phenylalanine aromatic ring breathing mode bands plotted against the ^{13}C-content.[24] However, SIRM has not been combined with SERS to date, which could be a highly attractive option to overcome existing sensitivity issues and limits of detection in SIRM.[10]

In this study we applied stable isotope Raman microspectroscopy (SIRM), resonance SIRM and SIRM in combination with surface-enhanced Raman scattering (SERS) to demonstrate the potential, the applicability and the limitations of these techniques for the analysis of ^{13}C-labeled single bacterial cells. A quantitative analysis of reference substances was performed to determine the minimal absolute amount of stable isotopes detectable with SIRM. ^{13}C-labeled glucose and phenylalanine were used as reference substances. Single cell Raman analyses were carried out for the *Deltaproteobacterium* spez. strain N47, a strictly anaerobic sulfate-reducer,[28] degrading the recalcitrant environmental pollutant naphthalene. Cells of *Geobacter metallireducens* GS-15, an iron-reducer capable of degrading aromatic pollutants and known for its large amount of *c* type cytochromes[29,30] were used for the testing of resonance Raman analysis. Due to its ease of handling and fast growth *E. coli* strain DSM 1116 was chosen as model biomass for our demonstration of SERS in combination with SIRM.

Experimental Section

Raman microspectroscopic analysis

A Lab-RAM HR Raman microscope (Horiba Scientific, Japan) with an integrated Olympus BXFM microscope was used for the Raman analysis. The measurements were carried out with a frequency-doubled Nd:YAG laser (532 nm, 8.4 mW at the sample) or a He-Ne-Laser (633 nm, 3.7 mW at the sample). The laser beam was focused onto the sample with a 100× objective (Olympus MPlan N, NA = 0.9). The full laser power and an acquisition time of 100 s were chosen for measurements of the reference compounds and strain N47. For SERS analysis of *E. coli,* the 633-nm laser was applied with a laser power of 0.037 mW or 0.0037 mW at the sample and an acquisition time of 1 s or 10 s. The characterization of *G. metallireducens* cells was carried out with a 532-nm laser, an acquisition time of 6 s (resonance Raman) or 100 s (normal Raman) and a laser power of 4.2 mW at the sample. The Raman scattering was collected in a 180° backscatter geometry. The Rayleigh scattering and the Anti-Stokes Raman scattering were removed by an edge filter. The Stokes Raman scattered light was passed through a diffraction grating (600 lines/mm) and a confocal pinhole (100 µm). Lateral and axial resolution was ca. 1 µm and ca. 2 µm, respectively. The signal was detected with a –72 °C-Peltier-cooled CCD detector. Usually the Raman spectra were recorded over a spectral range from 50 cm^{-1} to 4000 cm^{-1}. In contrast, the resonance Raman analyses of *G. metallireducens* were carried out in static mode (center at 944 cm^{-1}, spectral range from 50 cm^{-1} to 1750 cm^{-1}). The wavelength calibration was performed by focusing the laser beam on a silicon wafer with a 50× objective (Olympus MPlan N, NA = 0.75) and evaluating the first-order phonon band of silicon at 520.7 cm^{-1}. SERS samples were directly analyzed on glass slides. All other samples were measured on CaF_2 plates. With its sharp band at 320 cm^{-1}, CaF_2 was also used as an internal standard to ensure a proper calibration and correct the measured spectra if necessary.

Chemicals

L-phenylalanine ($C_9H_{11}NO_2$), $^{13}C_9$-^{15}N-L-phenylalanine ($^{13}C_9H_{11}{}^{15}NO_2$), D-glucose monohydrate ($C_6H_{12}O_6 \cdot H_2O$), $^{13}C_6$-D-glucose ($^{13}C_6H_{12}O_6$), sodium acetate ($C_2H_3NaO_2$), $^{13}C_2$-sodium acetate ($^{13}C_2H_3NaO_2$), $^{2}H_3$-sodium acetate ($C_2{}^{2}H_3NaO_2$), sodium bicarbonate ($NaHCO_3$), naphthalene ($C_{10}H_8$) and $^{13}C_{10}$-naphthalene ($^{13}C_{10}H_8$) were obtained from Sigma-Aldrich (Steinheim, Germany). Silver nitrate ($AgNO_3$) and sodium hydroxide solution 0.1 N (NaOH) were purchased from Carl Roth GmbH & Co. KG (Karlsruhe, Germany). Hydroxylammonium chloride ($NH_2OH \cdot HCl$) was obtained from Merck (Hohenbrunn, Germany). Glass slides (26 mm × 76 mm × 1 mm) were obtained from Carl Roth GmbH & Co. KG (Karlsruhe, Germany). CaF_2 single crystals (diameter 22 mm × 5 mm) were purchased from CRYSTAL GmbH (Berlin, Germany).

Scanning electron microscopy

Scanning electron microscopy (SEM) images of N47 cells (fixed in ethanol and dried on Si wafer) were obtained with a field emission scanning electron microscope (AURIGA 60-39-20,Carl Zeiss Microscopy GmbH, Germany) with an in-lens secondary electron detector (InLens, Carl Zeiss Microscopy GmbH, Germany).The sample was measured under vacuum (1.93×10^{-6} mbar) at an acceleration voltage of 30 kV, a probe current of 50 pA, and a working distance of 4.0 mm.

Preparation of isotopic mixtures of reference substances

Isotopic mixtures of $^{12}C/^{13}C$-glucose (0.1 M) were produced containing 1, 2, 4, 6, 8, 10, 20, 50, 60, 80, and 99% ^{13}C-glucose. To obtain a homogeneous alloy, 10 µL of each sample was spotted onto a CaF_2 single crystal and dried at room temperature overnight. The analyses were performed with a 532-nm and a 633-nm laser with acquisition times of 50 s and 100 s, respectively. The same procedure was applied for the preparation of $^{12}C/^{13}C$-phenylalanine mixtures (0.05 M) with 1, 5, 10, 15, 20, 30, 40, 50, 60, 80, and 98% ^{13}C-phenylalanine which were analyzed with the 633-nm laser and an acquisition time of 100 s.

Cultivation and preparation of bacteria, in situ *synthesis of colloidal silver nanoparticles*

The sulfate-reducing culture N47 was enriched from soil material of a contaminated aquifer near Stuttgart, Germany.[28] The strain was cultivated anaerobically in serum bottles containing hydrogen carbonate-buffered freshwater medium (pH 7.3) at 30 °C using naphthalene as carbon source and sulfate as electron acceptor.[31] The bottles were sealed with blue butyl stoppers (Glasgerätebau Ochs, Bovenden, Germany) and aluminum caps. Naphthalene was added as a 1.5% (w/v) solution in 2,2,4,4,6,8,8-heptamethylnonane (1 mL/50 mL culture volume). N47 cells were harvested and analyzed in the mid-exponential phase of growth. The samples were prepared according to Amann et al.[32] and Giovannoni et al.[33] with minor changes. 25 mL N47 culture were harvested (3739 g, 35 min) and washed in 1× phosphate-buffered saline (PBS, pH 7.4; 137 mM NaCl, 2.7 mM KCl, 8 mM $Na_2HPO_4 \cdot 2H_2O$, 1.5 mM KH_2PO_4) (1700 g, 10 min). Then, the cells were fixed with freshly prepared 4% para-formaldehyde (PFA in 1×PBS). One volume of PFA was added to 3 volumes of cell suspension and the mixture was incubated at 4 °C for 12 h. Afterwards, the cells were pelleted (1700 g, 10 min, 4 °C), washed with 1×PBS to remove residual PFA, centrifuged again and treated with an ethanol series (50%, 80%, absolute ethanol). Fixed cells in ethanol were stored at –20 °C. For Raman microspectroscopic studies 10 µL of the bacterial suspension were dropped onto a CaF_2 plate and was analyzed shortly after evaporation of the ethanol.

Geobacter metallireducens strain GS-15 (DSM 7210) was purchased from the Deutsche Sammlung von Mikroorganismen und Zellkulturen GmbH (Braunschweig, Germany). Microorganisms were cultivated under anoxic conditions in a minimal medium (DSMZ *Geobacter* medium 579) with DSMZ trace element solution SL10 (1 mL/L) and DSMZ 7 vitamin solution (0.5 mL/L).[34] Single substrates were added (^{12}C-acetate, 5 mM or ^{13}C-acetate, 5 mM or ^{2}H-acetate, 5 mM) and Fe(III) citrate (50 mM) was used as the electron acceptor. 40 mL of medium were dispensed into sterile 50 mL bottles. The bottles were flushed with a mixture of N_2 and CO_2 (80% : 20%) and sealed with butyl rubber stoppers. All incubations were performed at 30 °C in the dark. Cells from the third transfer on ^{13}C-acetate and ^{2}H-acetate were used for Raman analysis. Fixation in PFA and the preparation for Raman microspectroscopy were done as for strain N47 (see above).

Shock frozen *E. coli* strain DSM 1116 strains were purchased from DSM Nutritional Products GmbH (Grenzach, Germany). The cells were transferred into 250 mL shake flaks containing 25 mL M9 minimal medium[35,36] with trace element solutions (mg/l): EDTA, 15; $CaCl_2$, 5; $MgSO_4$, 5; $FeSO_4 \cdot 7H_2O$, 3; H_3BO_3, 28; $MnCl_2 \cdot 4H_2O$, 18; $ZnSO_4 \cdot 7H_2O$, 2; $Na_2MoO_4 \cdot 2H_2O$, 4; $CuSO_4 \cdot 5H_2O$, 0.8; $Co(NO_3)_2 \cdot 6H_2O$, 0.5. The flasks were incubated overnight at 100 rpm and 37 °C with 0.4% (w/v) ^{12}C- or ^{13}C-glucose as well as a 1:1 mixture of ^{12}C- and ^{13}C-glucose.

For SERS analysis a slightly modified procedure for *in situ* preparation of AgNP was used.[12] Briefly, ten milliliters of bacteria were harvested and washed twice in Milli-Q-water (3328 g, 10 min at 4 °C), 1 mL of the liquid was pelleted and resuspended in 180 µL of hydroxylammonium chloride solution (1.67 mM) containing NaOH (3.3 mM), resulting in a pH of 7.0. Afterwards, 20 µL of silver nitrate solution (10 mM) was rapidly pipetted into the mixture and mixed by inverting. After an interaction time of 1 hour at 4 °C, 5 µL of the bacterial sample were pipetted onto a glass slide. The samples were analyzed after drying for 1 hour.

Results and discussion

Raman analysis of reference compounds and mixtures

In order to explore the potential of stable isotope Raman microspectroscopy (SIRM) for quantitative analysis of isotopic labeling, mixture series of reference substances were analyzed. The Raman spectra and a brief band assignment of $^{12}C/^{13}C$-phenylalanine, $^{12}C/^{13}C$-glucose and $^{12}C/^{13}C/^{2}H$-sodium acetate can be found in the supporting information (SI) (Fig. S-1).

First, the ratio of the intensities for ^{13}C- and ^{12}C-phenalaline peaks (965 cm^{-1} and 1002 cm^{-1}, respectively) was plotted against the $^{13}C/^{12}C$-ratio. The limits of detection (LOD) with the 3-σ criterion of 9.5% ^{13}C-content for 965 cm^{-1} / 1002 cm^{-1} and 6.5% ^{13}C-content for 1550 cm^{-1} / 1604 cm^{-1} (Fig. S-2) were achieved. Second, a multivariate calibration method, called partial least squares (PLS), was used to determine the ^{13}C-content. Figure S-3 illustrates the least squares calibration of $^{12}C/^{13}C$-phenylalanine. A more sensitive limit of detection (LOD) of 2.8% ^{13}C-content was calculated for this approach. Finally, the minimal absolute amount of the ^{13}C-compound detectable in the laser spot was determined. With acquisition times of 100 s per spectra 0.148 ± 0.008 pg and 0.327 ± 0.017 pg ^{13}C-glucose could be detected for the 532 nm laser and the 633 nm laser, respectively. Detailed information about these three methods can be found in the SI.

The limits of detection determined here for pure compounds suggest that in feeding experiments with stable isotope-labeled compounds already very small amounts of incorporation will be detectable and quantifiable.

Raman analysis of isotopically labeled N47 cells

Here, we applied SIRM for analysis of carbon incorporation into the biomass of the naphthalene-degrading strain N47. Strain N47 grows extremely slow but is still the best studied microorganisms degrading naphthalene in the absence of molecular oxygen. The initial degradation step in anaerobic naphthalene degradation is a carboxylation to 2-naphthoic acid.[37] Fully labeled ^{13}C-naphthalene and non-labeled hydrogen carbonate were used in the culture medium suggesting a respective ^{12}C/^{13}C peak pattern of the phenylalanine bands. Optical microscope and SEM images of single N47 cells show a length of about 1 – 2 µm (Fig. 1a, b). Minor but negligible variations in the Raman spectra of individual cells were found, most likely due to slightly different cell morphology or metabolic states. Still, a very good reproducibility of Raman microspectroscopic spectra of different N47 cells cultivated with ^{12}C-napthalene was revealed (Fig. 1c). Spectra of ^{12}C-N47 cells and N47 cells cultivated with fully labeled ^{13}C-naphthalene show differences in the region of the phenylalanine marker band at 1001 cm^{-1} (Fig. 1d). The four peaks at 1001 cm^{-1}, 990 cm^{-1}, 978 cm^{-1}, and 968 cm^{-1} can be assigned to the different isotopologues of phenylalanine with 0, 2, 4 or 6 ^{13}C-atoms in the aromatic ring.[26] Thus the isotopic labeling of N47 was clearly recovered in SIRM spectra, however fully labeled biomass was not detected. Moreover, the analysis of cells cultivated with ^{12}C-napthalene and ^{13}C-labeled hydrogen carbonate also showed a partial red-shift of the phenylalanine band to 990 cm^{-1} (data not shown). This suggests a significant contribution of hydrogen carbonate from the medium to biomass buildup during naphthalene degradation, which is consistent with the high ratios of heterotrophic CO_2-fixation already reported for other strictly anaerobic aromatics degraders detected via distinct stable isotope probing methodologies.[38,39] Due to cost reasons, the pre-culture of the analyzed cells was grown in ^{12}C-naphthalene. Therefore a remaining contribution of ^{12}C-naphthalene or its intermediates to biomass buildup cannot be excluded. However, the cultures were always grown with 10% inoculum. Thus, a carryover of biomass should either result in less than 10% of non-labeled cells if the majority of the inoculated cells did not grow. Alternatively, if all cells inoculated into the ^{13}C-naphthalene containing medium grew, the carryover from the pre-culture could only account for less than 10% of the biomass of each cell. The data acquired for strain N47 showed that SIRM is a suitable method for analysis of isotopic labeling patterns in microorganisms at single cell level. This even holds for such extremely slow growing cultures with incubation times of longer than 2 months. If the extent of label incorporation into phenylalanine is representative of the total biomass one could also deduce the absolute amount of label uptake. This would allow for determining e.g. the extent of heterotrophic CO_2-fixation or other types of mixed substrate utilization on single cell level.

However, due to the low quantum efficiency of the Raman effect (typically $10^{-6} – 10^{-8}$), SIRM suffers from a limited sensitivity making SIRM analysis rather time consuming (e.g. acquisition time of 100 s was used in this study resulting in ca. 10 min for one spectrum in region 50 cm^{-1} – 4000 cm^{-1}).

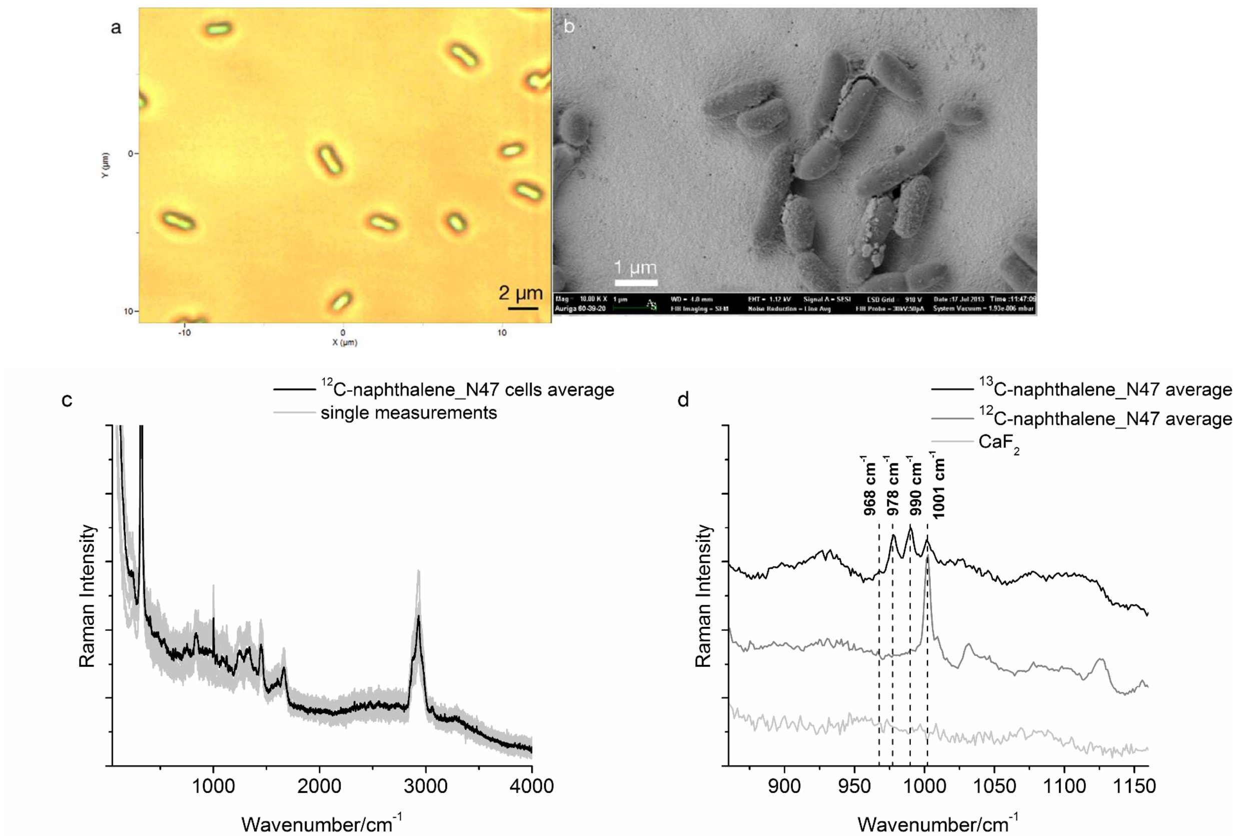

Figure 1. Optical microscope (a) and (b) scanning electron microscope (SEM) images of single cells of strain N47; (c) single cell measurements of ^{12}C-N47 (six replicates) and their average spectrum show very good reproducibility; (d) Raman spectra of N47 cells cultivated with either ^{12}C-napthalene or ^{13}C-naphthalene and the characteristic red-shift of the phenylalanine band. The four highlighted peaks were assigned to four different isotopologues of phenylalanine.

Resonance Raman analysis of G. metallireducens

We tested to which extent the application of a resonance Raman effect can help to overcome the limited sensitivity of SIRM analysis of single cells. With its large amount of *c* type cytochromes[29,30] *G. metallireducens* is an optimal microorganism to study the uptake of stable isotope marked substances into bacterial cells with short acquisition times. To obtain resonance Raman bands a 532-nm laser was used for the analysis of cells of *G. metallireducens*. Notably, the photobleaching effect of cytochrome *c* limited the maximum acquisition time.[16] After 7 – 10 s of laser exposition time the cytochrome *c* in the cells was completely bleached and the resonance Raman bands vanished (Fig. 2a). Although a measurement time as short as 1 s would be clearly possible for this type of cells, an acquisition time of 6 seconds was chosen to collect as much cytochrome *c* signal as possible to obtain resonance Raman bands with good signal-to-noise ratio. The most prominent resonance Raman bands were found at 746 cm^{-1}, 1128 cm^{-1}, 1311 cm^{-1} and 1583 cm^{-1}. They were assigned to porphyrin breathing, C–N stretching modes, C–H bending modes, and anti-symmetric C–C stretching, respectively.[16] The reproducibility of a single cell measurement of *G. metallireducens* over 6 s (resonance Raman spectra dominated by cytochrome *c* bands, Fig. 2b) and 100 s (Raman spectra showing whole-organism fingerprint of bacteria, Figure 2c) acquisition time were very good. Only minor differences between the spectra were observed, caused by a slightly different cell composition due to natural variances. Differences in relative intensities of the resonance Raman bands in figure 2b can be accounted to changes in oxidation states of cytochrome *c*.[40,41]

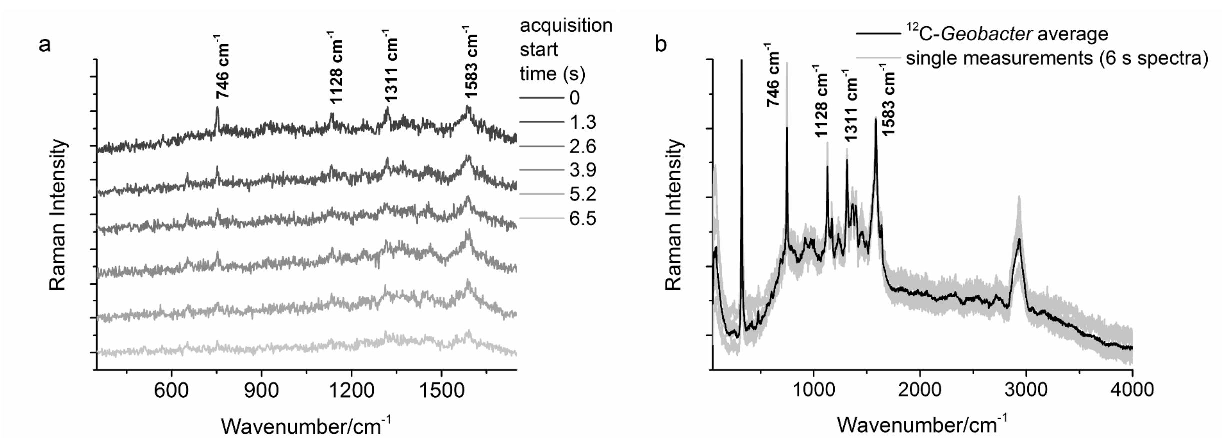

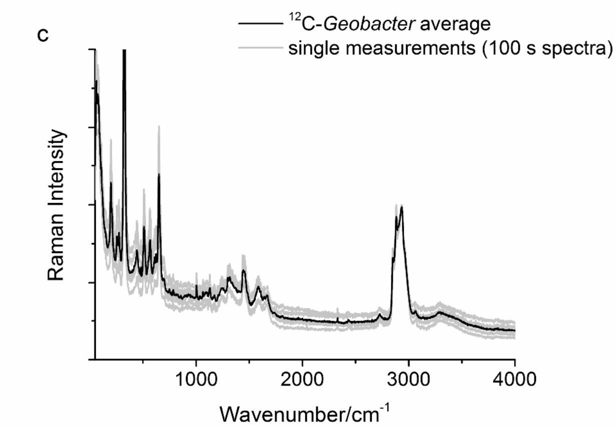

Figure 2. Resonance Raman microscopy spectra of single cells of *G. metallireducens*. (a) Time series of 6 consecutive spectra of one single cell of *G. metallireducens* with an acquisition time of 1 s per spectrum, 0.3 s time difference between each spectrum, and a laser power of 4.2 mW. The photobleaching effect due to the laser radiation is clearly visible; (b) overlays of spectra of individual cells of *G. metallireducens* taken for 6 s and (c) 100 s.

In order to study the uptake of stable isotopes into the cell, *G. metallireducens* cultivated with ^{12}C-acetate were compared to *G. metallireducens* grown with fully labeled ^{13}C-acetate or fully deuterated acetate. A significant red-shift of up to 13 cm^{-1} of the cytochrome *c* bands could be found for ^{13}C-acetate grown cells of *G. metallireducens* (Fig. 3). No noteworthy red-shift (1 cm^{-1}) was observed for the porphyrin breathing, indicating that no or only few ^{13}C-atoms were involved in this mode. However, the peaks at 1128 cm^{-1}, 1311 cm^{-1} and 1583 cm^{-1} (for ^{12}C-*G. metallireducens*) showed a clear red-shift of about 5 cm^{-1} to 1123 cm^{-1}, 1307 cm^{-1} and 1577 cm^{-1} (in ^{13}C-*G. metallireducens*). The strongest red-shift of around 13 cm^{-1} could be found for another anti-symmetric C–C stretching mode[42] with its band at 1638 cm^{-1} in ^{12}C-*G. metallireducens*. This overall relatively small red-shift indicates an incomplete replacement of ^{12}C with ^{13}C during cultivation. To verify this, we analyzed ^{13}C-labeled *G. metallireducens* after photobleaching with an acquisition time of 100 s to obtain whole-organism fingerprint spectra (Fig. 4a). With fully ^{13}C-labeled cells the phenylalanine marker band should only show one peak at 968 cm^{-1}. But in fact we see bands at 978 cm^{-1}, 990 cm^{-1} and 1001 cm^{-1}. These bands are from isotopologues of phenylalanine with less than 6 ^{13}C-atoms in the aromatic ring structure[26] and clearly show that we indeed have no full ^{13}C-labeling. The remaining ^{12}C should be due to the uptake of $^{12}CO_2$ from atmosphere and/or from $NaHCO_3$ buffer by cells into their biomass. However, the observed shift is perfectly reproducible (for example with a deviation of ± 0.5 cm^{-1} for the band at 1577 cm^{-1}). Therefore the detection and differentiation of the ^{13}C-labeled cells was possible.

For deuterated acetate-cultivated bacteria, a shift of the band at 1311 cm^{-1} (C–H bending) was expected but could not be observed. Therefore, it can be assumed that ^{2}H was not incorporated into cytochrome *c*. To see whether deuterium was incorporated into other constituents of the biomass and particularly at phenylalanine marker band an acquisition time of 100 s was chosen to obtain whole-organism fingerprint spectra with a good signal-to-noise ratio and a complete photobleaching of the resonance Raman peaks. The C–^{1}H stretching band at around 2900 cm^{-1} was partially red-shifted to around 2200 cm^{-1} (C–^{2}H stretching) (Fig. 4b). The region from ~1800 cm^{-1} to ~2800 cm^{-1} is the so-called "Raman-silent" region[43], meaning usually no Raman bands of organic compounds and especially no bands of non-deuterated constituents can be found here. This region allows for a selective detection of deuterated species in human cells.[44] The comparison of the integral of both peaks suggests a deuterium-content in *G. metallireducens* cells around 20%. One explanation for this low deuterium content may be the substitution of deuterium with protons from water. The phenylalanine marker peak was partially red-shifted from 1001 cm^{-1} to 988 cm^{-1}, 975 cm^{-1}, and 960 cm^{-1}. The peak at 960 cm^{-1} is assigned to the fully deuterated phenylalanine ring breathing mode.[45,46] Therefore we suppose that, analogous to the peak pattern observed for ^{13}C-incorporation into N47 cells (see above), also isotopologues of phenylalanine with less than 5 deuterium atoms produce the peaks at 988 cm^{-1} and 975 cm^{-1}. Probably, the peak at 988 cm^{-1} derives from phenylalanine with only one deuterium atom situated at the ring (analogous to the red-shift of this band in toluene from 1004 cm^{-1} to 987 cm^{-1} for 4-$^{2}H_1$-toluene[47]).

Our data reveal that resonance Raman spectroscopy provides fast and sensitive analysis of ^{13}C-incorparation into biomass of chromophore-containing microorganisms. The application of deuterated substrates does not affect the resonance Raman bands of the chromophore but produces new peaks in the phenylalanine region and in the otherwise Raman-silent region between 2000 and 2500 cm^{-1}. Thus, deuterium-labeling can be an attractive alternative to ^{13}C-labeling for tracing incorporation of stable isotope-labeled substrates into biomass on single cell level. The application of SIRM for the analysis of chromophore-containing bacteria can provide complementary information on the chromophore (e.g. cytochrome *c*) and the whole-organism fingerprint of a single bacterium achieved before and after photobleaching, respectively.

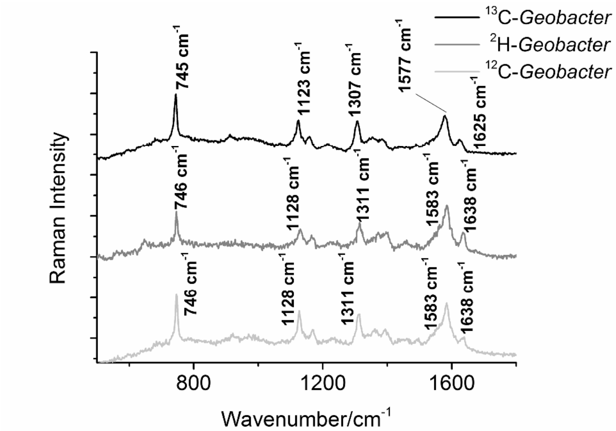

Figure 3. Resonance Raman spectra of single cells of *G. metallireducens* cultivated with unlabeled acetate, deuterated acetate or ^{13}C-acetate in the fingerprint region. An acquisition time of 6 s was used for taking the spectra.

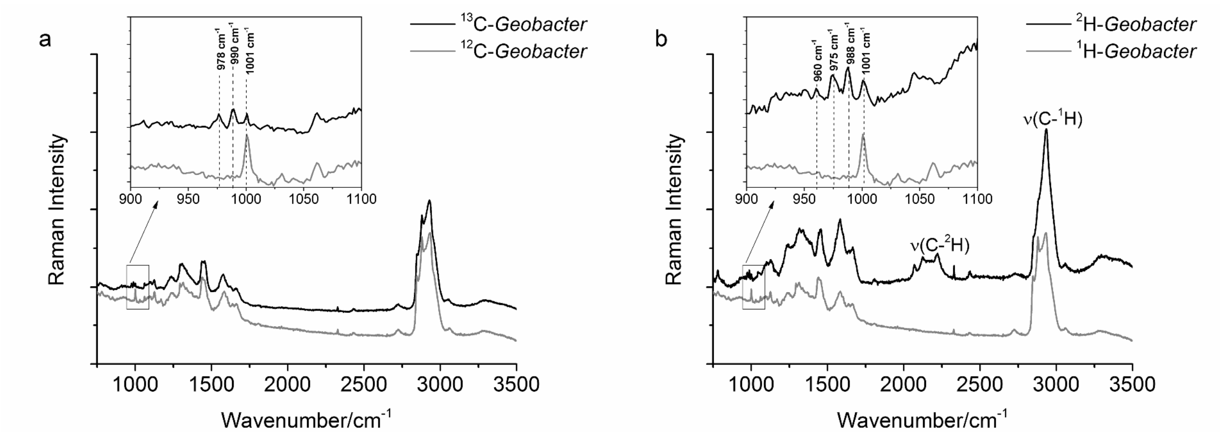

Figure 4. Stable isotope Raman spectra of single cells of *G. metallireducens* cultivated with unlabeled acetate and (a) ^{13}C-labeled acetate or (b) deuterated acetate; inserts: zoom of the phenylalanine region around 1000 cm^{-1} and the peak pattern of isotopologues. The ^{2}H-isotopologues can be found at 960 cm^{-1}, 975 cm^{-1}, 988 cm^{-1} and 1001 cm^{-1}, the ^{13}C- isotopologues at 978 cm^{-1}, 990 cm^{-1} and 1001 cm^{-1}. An acquisition time of 100 s was used for all spectra.

SERS analysis of E. coli strain DSM 1116

Surface-enhanced Raman scattering (SERS) in combination with RM is often applied in order to achieve rapid and sensitive analysis of single bacterial cells.[5-7] We therefore also applied SERS to enhance the Raman signals of unlabeled and ^{13}C-labeled *E. coli* cells. An overall SERS enhancement of about 10^4 was found for C–H stretching modes at around 2900 cm^{-1} comparing spectra of individual *E. coli* cells cultivated with ^{12}C- or ^{13}C-glucose, respectively. The SERS spectra of ^{12}C- and ^{13}C-cells showed a high reproducibility (Fig. 5a, b). In particular, a very sharp marker band at 733 cm^{-1} for ^{12}C-*E. coli* was found, which can be assigned to adenine, adenine derivatives[48,49] or COO^- deformation modes (e.g. in polyanionic carbohydrates)[50]. Since this band did not vanish if using a high enough laser power leading to appearance of soot-like bands due to thermal decomposition of the biomass, the band more likely originated from adenine. According to Kahraman et al. this band "could be due to molecules possessing the adenine moiety in their structure, located on or in the cell wall structure. Examples of adenine derivatives or adenine-containing molecules include DNA, RNA, RF, FAD, NAD, NADH, ADP, or ATP"[49]. This prominent band has a high intensity in relation to the rest of the spectrum and even with a low signal-to-noise ratio of the whole spectrum, this band was easily detectable. Therefore, this band is a very good novel candidate as a marker of isotope incorporation in biomass in SERS-SIRM. And in fact a clear red-shift (13 cm^{-1}) of the SERS marker band at 733 cm^{-1} for ^{12}C-*E. coli* to 720 cm^{-1} for ^{13}C-*E. coli* and red-shift of 7 cm^{-1} to 726 cm^{-1} for 50% ^{13}C-*E. coli* was observed (Fig. 5c). This enables a rapid detection and a differentiation of normal ^{12}C-*E. coli* and stable isotope labeled *E. coli* cells by means of SERS. With this increased sensitivity it would be possible to use stable-isotope labeling in combination with SERS as a tool for the characterization of the isotopic labeling and molecular composition of microorganisms at single cell level in a short time. In environmental microbiology this approach can open new possibilities for sensitive analysis of high variety of microbiological processes, e.g. degradation of pollutants, carbon flow and metabolic pathways. To our knowledge, this is the first demonstration of reproducible SERS measurements of single bacterial cells labeled with stable isotopes.

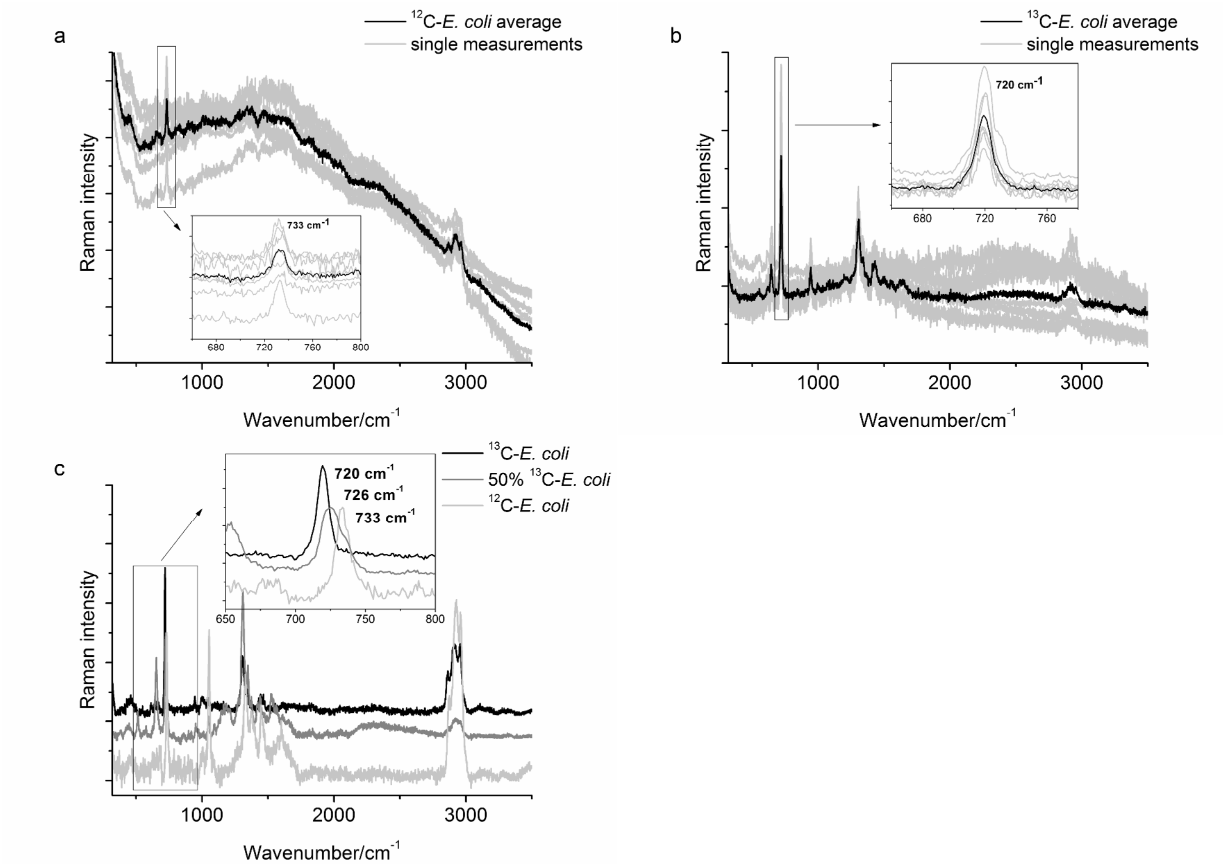

Figure 5. SERS measurements of single *E. coli* cells grown with non-labeled ^{12}C-glucose (a), or ^{13}C-labeled glucose cells (b). (c) Overlay of SERS spectra of ^{13}C-, 50% ^{13}C- and ^{12}C-*E. coli* cells showing the red-shift (13 cm^{-1}) of the SERS marker band at 733 cm^{-1} for ^{12}C-*E. coli* to 720 cm^{-1} for ^{13}C-*E. coli* in baseline-corrected SERS spectra. The band for 50% ^{13}C-labeled *E. coli* can be found at 726 cm^{-1}. The band at 1055 cm^{-1} is assigned to silver nanoparticles [11]; inserts: zoom to the region of the bands at 733 cm^{-1}, 726 cm^{-1}and 720 cm^{-1}.

Conclusions

In this study, we explored the potential of stable isotope Raman microspectroscopy for the nondestructive quantitative and spatially-resolved analysis of incorporation of stable isotope-labeled compounds into microbial biomass. Figure 6 presents schematically our results. Using ^{12}C- and ^{13}C-glucose and phenylalanine as reference compounds we showed that the minimal absolute amount of ^{13}C-glucose which could be detected in ^{12}C-glucose via SIRM (λ_0 = 532 nm) is around 0.1 pg for a laser spot with a diameter of 721 nm. A linear relation between the ratio of a selected peak at its ^{13}C and ^{12}C maxima and the ^{13}C/^{12}C-ratio for ^{12}C/^{13}C-mixtures of reference substances with a high degree of correlation was demonstrated. The partial least squares calibration method for ^{12}/^{13}C-glucose and phenylalanine mixtures yielded a linear trend with limit of detection down to 3% isotope enrichment. Such a good detection limit allows for a very sensitive and quantitative analysis of stable isotope labeling of microorganisms compared to other methods such as nucleic acid based stable isotope probing (SIP).

The SIRM characterization of ^{13}C-labeled N47 cells confirmed the peak pattern from isotopologues of phenylalanine described by Li et al.[26] for *E. coli* cells cultivated with ^{12}C/^{13}C-glucose mixtures, albeit for a strict anaerobe growing on ^{13}C-naphthalene. Furthermore, our results suggest an incorporation of hydrogen carbonate from the medium into biomass build-up during growth on naphthalene by strain N47. Resonance SIRM of *G. metallireducens* containing cytochrome *c* with an acquisition time of 6 s was successfully established to observe the ^{13}C-uptake of single bacterial cells. Measurement times as short as 1 s thus become possible, enabling a fast distinction between ^{12}C-and ^{13}C-labeled bacteria. The chromophore-derived information obtained via resonance SIRM can be successfully complemented with whole-organism Raman fingerprints of microorganisms achieved via SIRM after photobleaching. For ^{2}H-labeled cells the "Raman-silent" region with the ν (C–^{2}H) mode ~2200 cm^{-1} enabled a definite discrimination between normal ^{12}C-cells and ^{2}H-labeled bacteria. Although the deuterium content in the cells was found to be quite low (~20%), a clear peak pattern from different isotopologues of phenylalanine was shown for ^{2}H-labeled cells. Thus, we can show that deuterium labeling can provide an alternative to ^{13}C-labeling of biomass and Raman spectroscopy. With this knowledge a differentiation between normal ^{12}C-, ^{2}H-, and ^{13}C-labeled cells is clearly possible. Ultimately, SERS studies on *E. coli* cultivated with ^{12}C- and ^{13}C-glucose were performed. A very sharp marker band at 733 cm^{-1} for ^{12}C-*E. coli* was found which can be assigned to adenine or adenine-containing molecules .[48,49] It was clearly red-shifted to 720 cm^{-1} in ^{13}C-*E. coli* cells. With an overall enhancement factor of around 10^4, a rapid detection of stable isotope labeled *E. coli* by means of SERS becomes thus possible. To our knowledge these are the first reproducible SERS data of stable isotope labeled microorganisms, which can have significant implications for the use of Raman microspectroscopy in environmental microbiology because it opens a new variety of applications which have not been possible so far, due to limited sensitivity.

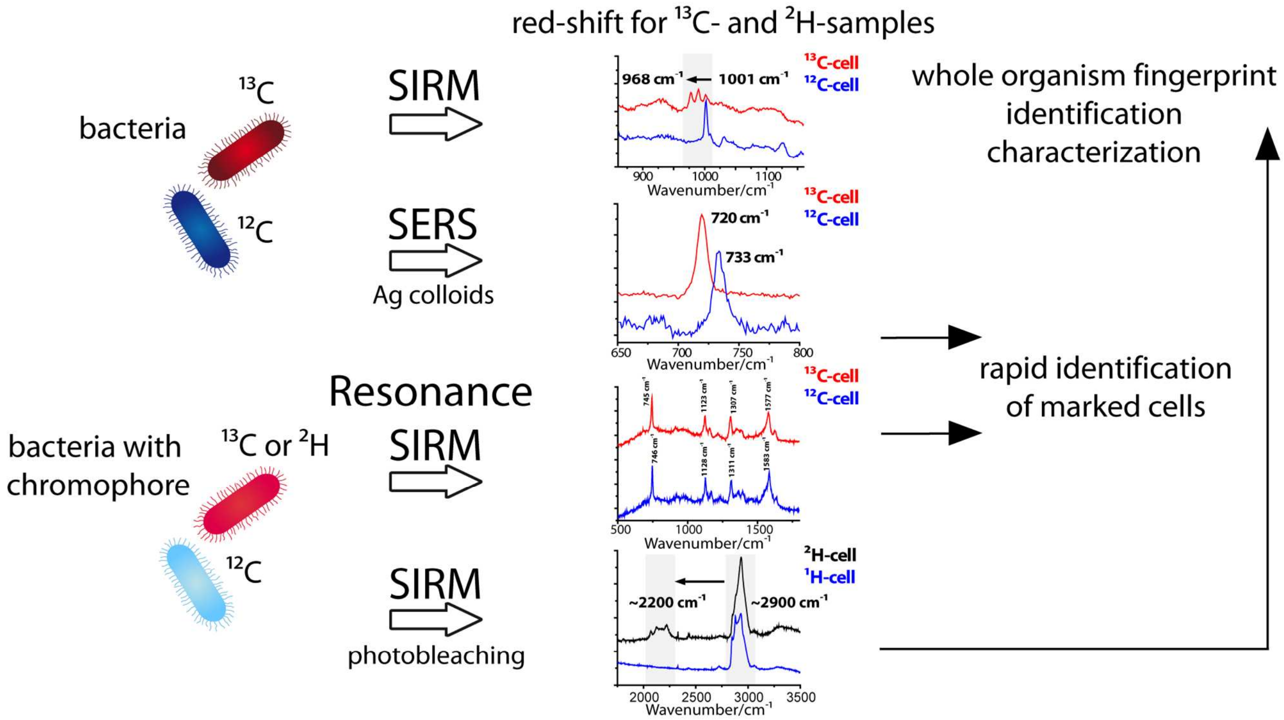

Figure 6. Scheme of this study with focus on the nondestructive quantitative and spatially-resolved analysis of incorporation of stable isotope-labeled compounds into microbial biomass.

Associated content

Supporting information as mentioned in the text. This material is available free of charge via the Internet at http://pubs.acs.org.

Acknowledgements

The authors gratefully acknowledge the financial support of the Helmholtz Wasserzentrum München (HWZM) within the Helmholtz Water Network. We want to thank Andreas Schertel, Carl Zeiss Microscopy GmbH, for conducting the SEM measurements of bacterial cells and providing the SEM images. We thank Andreas Kunze, Haibo Zhou, Christoph Haisch and Alexandra Wiesheu for help, valuable comments and suggestions.

References

(1) Huang, W. E.; Griffiths, R. I.; Thompson, I. P.; Bailey, M. J.; Whiteley, A. S. *Anal. Chem.* **2004**, *76*, 4452-4458.
(2) Harz, M.; Rösch, P.; Popp, J. *Cytometry, Part A* **2009**, *75A*, 104-113.
(3) Le Ru, E. C.; Etchegoin, P. G. *Annu. Rev. Phys. Chem.* **2012**, *63*, 65-87.
(4) Etchegoin, P. G.; Le Ru, E. C. *Phys. Chem. Chem. Phys.* **2008**, *10*, 6079-6089.
(5) Jarvis, R. M.; Goodacre, R. *Chem. Soc. Rev.* **2008**, *37*, 931-936.
(6) Sengupta, A.; Mujacic, M.; Davis, E. J. *Anal. Bioanal. Chem.* **2006**, *386*, 1379-1386.
(7) Liu, Y.; Chen, Y.-R.; Nou, X.; Chao, K. *Appl. Spectrosc.* **2007**, *61*, 824-831.
(8) Efrima, S.; Zeiri, L. *J. Raman Spectrosc.* **2009**, *40*, 277-288.
(9) Kahraman, M.; Yazici, M. M.; Sahin, F.; Bayrak, O. F.; Culha, M. *Appl. Spectrosc.* **2007**, *61*, 479-485.
(10) Wang, Y.; Ji, Y.; Wharfe, E. S.; Meadows, R. S.; March, P.; Goodacre, R.; Xu, J.; Huang, W. E. *Anal. Chem.* **2013**.
(11) Chao, Y.; Zhang, T. *Anal. Bioanal. Chem.* **2012**, *404*, 1465-1475.
(12) Zhou, H.; Yang, D.; Ivleva, N. P.; Mircescu, N. E.; Niessner, R.; Haisch, C. *Anal. Chem.* **2014**, *86*, 1525-1533.
(13) Spiro, T. G.; Strekas, T. C. *J. Am. Chem. Soc.* **1974**, *96*, 338-345.
(14) Salama, S.; Spiro, T. G. *J. Raman Spectrosc.* **1977**, *6*, 57-60.
(15) Lutz, M. *J. Raman Spectrosc.* **1974**, *2*, 497-516.
(16) Paetzold, R.; Keuntje, M.; Theophile, K.; Mueller, J.; Mielcarek, E.; Ngezahayo, A.; Anders-von Ahlften, A. *J. Microbiol. Methods* **2008**, *72*, 241-248.
(17) Li, M.; Canniffe, D. P.; Jackson, P. J.; Davison, P. A.; FitzGerald, S.; Dickman, M. J.; Burgess, J. G.; Hunter, C. N.; Huang, W. E. *ISME J.* **2012**, *6*, 875-885.
(18) Palings, I.; Pardoen, J. A.; Van den Berg, E.; Winkel, C.; Lugtenburg, J.; Mathies, R. A. *Biochemistry* **1987**, *26*, 2544-2556.
(19) Copeland, R. A.; Spiro, T. G. *J. Phys. Chem.* **1986**, *90*, 6648-6654.
(20) Palonpon, A. F.; Ando, J.; Yamakoshi, H.; Dodo, K.; Sodeoka, M.; Kawata, S.; Fujita, K. *Nat. Protoc.* **2013**, *8*, 677-692.
(21) Li, M.; Ashok, P. C.; Dholakia, K.; Huang, W. E. *J. Phys. Chem. A* **2012**, *116*, 6560-6563.
(22) López-Díez, E. C.; Goodacre, R. *Anal. Chem.* **2003**, *76*, 585-591.
(23) Neugebauer, U.; Schmid, U.; Baumann, K.; Ziebuhr, W.; Kozitskaya, S.; Deckert, V.; Schmitt, M.; Popp, J. *ChemPhysChem* **2007**, *8*, 124-137.
(24) Huang, W. E.; Stoecker, K.; Griffiths, R.; Newbold, L.; Daims, H.; Whiteley, A. S.; Wagner, M. *Environ. Microbiol.* **2007**, *9*, 1878-1889.
(25) Haider, S.; Wagner, M.; Schmid, M. C.; Sixt, B. S.; Christian, J. G.; Häcker, G.; Pichler, P.; Mechtler, K.; Müller, A.; Baranyi, C.; Toenshoff, E. R.; Montanaro, J.; Horn, M. *Mol. Microbiol.* **2010**, *77*, 687-700.
(26) Li, M.; Huang, W. E.; Gibson, C. M.; Fowler, P. W.; Jousset, A. *Anal. Chem.* **2012**, *85*, 1642-1649.
(27) Noothalapati, H.; Shigeto, S. *Anal. Chem.* **2014**, *86*, 7828-7834.
(28) Meckenstock, R. U.; Annweiler, E.; Michaelis, W.; Richnow, H. H.; Schink, B. *Appl. Environ. Microbiol.* **2000**, *66*, 2743-2747.
(29) Butler, J.; Young, N.; Lovley, D. *BMC Genomics* **2010**, *11*, 40.
(30) Aklujkar, M.; Krushkal, J.; DiBartolo, G.; Lapidus, A.; Land, M.; Lovley, D. *BMC Microbiol.* **2009**, *9*, 109.

(31) Annweiler, E.; Michaelis, W.; Meckenstock, R. U. *Appl. Environ. Microbiol.* **2002**, *68*, 852-858.
(32) Amann, R. I.; Binder, B. J.; Olson, R. J.; Chisholm, S. W.; Devereux, R.; Stahl, D. A. *Appl. Environ. Microbiol.* **1990**, *56*, 1919-1925.
(33) Giovannoni, S. J.; DeLong, E. F.; Olsen, G. J.; Pace, N. R. *J. Bacteriol.* **1988**, *170*, 720-726.
(34) Marozava, S.; Röling, W. F. M.; Seifert, J.; Küffner, R.; von Bergen, M.; Meckenstock, R. U. *Syst. Appl. Microbiol.* **2014**, *37*, 277-286.
(35) Green, M. R.; Sambrook, J. *Molecular cloning : a laboratory manual*; Cold Spring Harbor Laboratory Press: Cold Spring Harbor, N.Y, 2012.
(36) Sabri, S.; Nielsen, L. K.; Vickers, C. E. *Appl. Environ. Microbiol.* **2013**, *79*, 478-487.
(37) Mouttaki, H.; Johannes, J.; Meckenstock, R. U. *Environ. Microbiol.* **2012**, *14*, 2770-2774.
(38) Winderl, C.; Penning, H.; Netzer, F. v.; Meckenstock, R. U.; Lueders, T. *ISME J* **2010**, *4*, 1314-1325.
(39) Taubert, M.; Vogt, C.; Wubet, T.; Kleinsteuber, S.; Tarkka, M. T.; Harms, H.; Buscot, F.; Richnow, H.-H.; von Bergen, M.; Seifert, J. *ISME J* **2012**, *6*, 2291-2301.
(40) Spiro, T. G.; Strekas, T. C. *Proc. Natl. Acad. Sci. U.S.A.* **1972**, *69*, 2622-2626.
(41) Cartling, B. *Biophys. J.* **1983**, *43*, 191-205.
(42) Li, X. Y.; Czernuszewicz, R. S.; Kincaid, J. R.; Su, Y. O.; Spiro, T. G. *J. Phys. Chem.* **1990**, *94*, 31-47.
(43) Etchegoin, P. G.; Le Ru, E. C.; Meyer, M. *J. Am. Chem. Soc.* **2009**, *131*, 2713-2716.
(44) van Manen, H.-J.; Lenferink, A.; Otto, C. *Anal. Chem.* **2008**, *80*, 9576-9582.
(45) Overman, S. A.; Thomas, G. J. *Biochemistry* **1995**, *34*, 5440-5451.
(46) Overman, S. A.; Thomas, G. J. *J. Raman Spectrosc.* **1998**, *29*, 23-29.
(47) Wilmshurst, J. K.; Bernstein, H. J. *Can. J. Chem.* **1957**, *35*, 911-925.
(48) Maquelin, K.; Kirschner, C.; Choo-Smith, L. P.; van den Braak, N.; Endtz, H. P.; Naumann, D.; Puppels, G. J. *J. Microbiol. Methods* **2002**, *51*, 255-271.
(49) Kahraman, M.; Keseroglu, K.; Culha, M. *Appl. Spectrosc.* **2011**, *65*, 500-506.
(50) Ivleva, N. P.; Wagner, M.; Szkola, A.; Horn, H.; Niessner, R.; Haisch, C. *J. Phys. Chem. B* **2010**, *114*, 10184-10194.

for TOC only

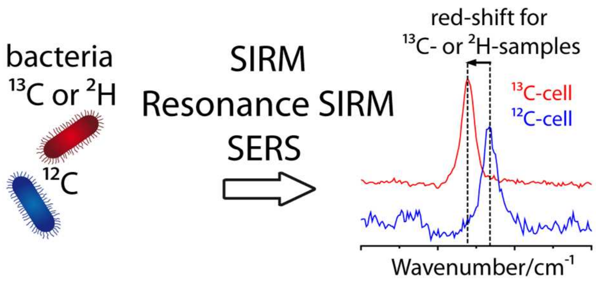
bacteria
13C or 2H
12C
SIRM
Resonance SIRM
SERS
red-shift for
13C- or 2H-samples
13C-cell
12C-cell
Wavenumber/cm-1

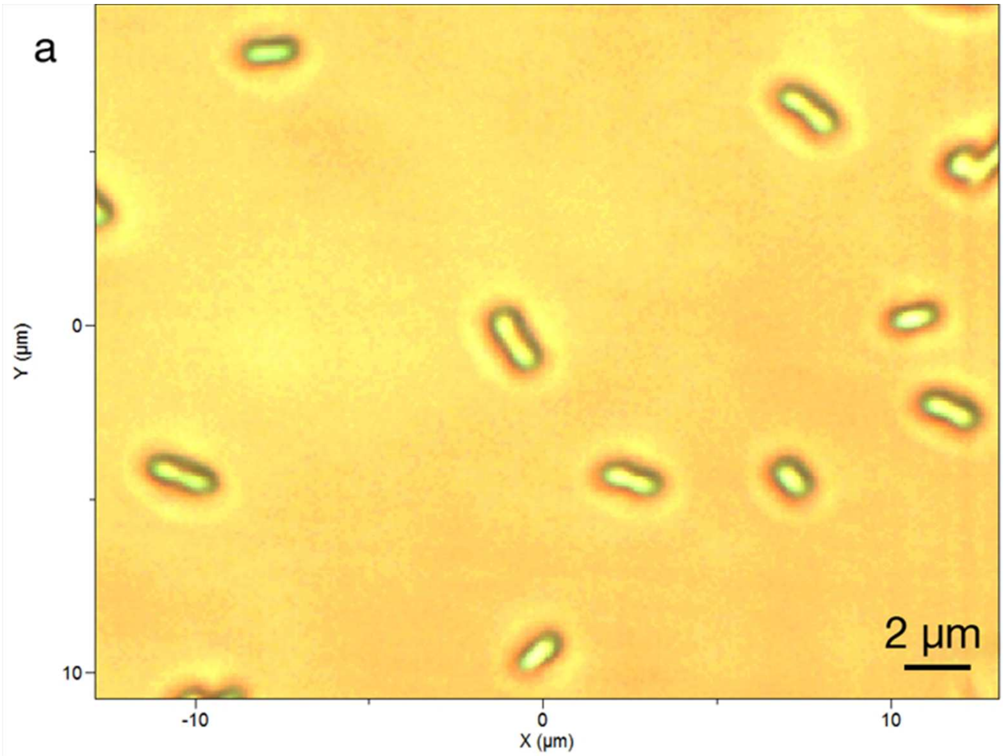

Figure 1 a
60x45mm (300 x 300 DPI)

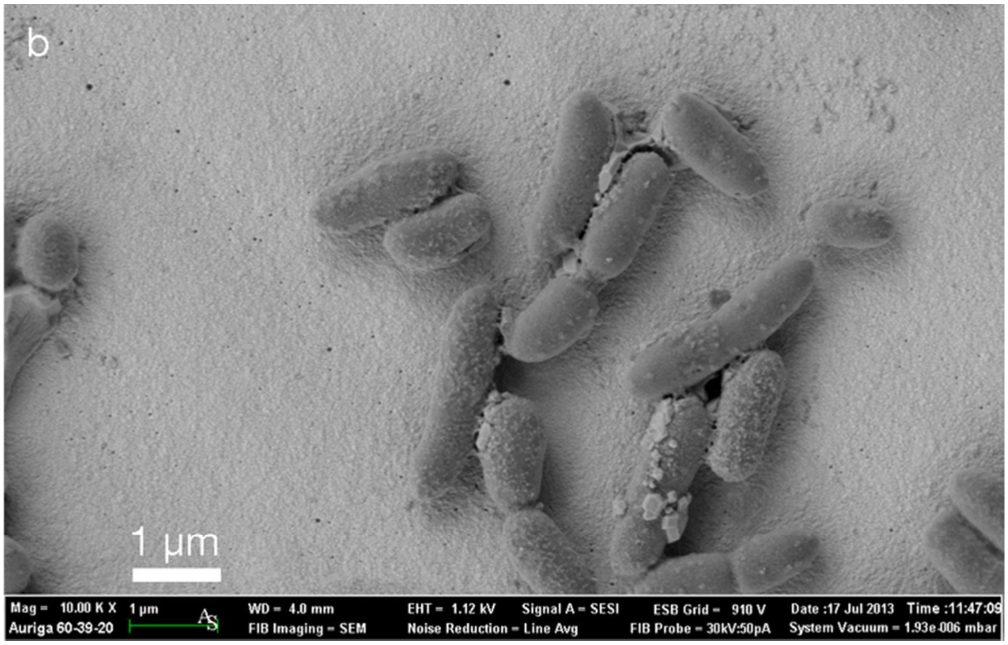

Figure 1 b
64x40mm (300 x 300 DPI)

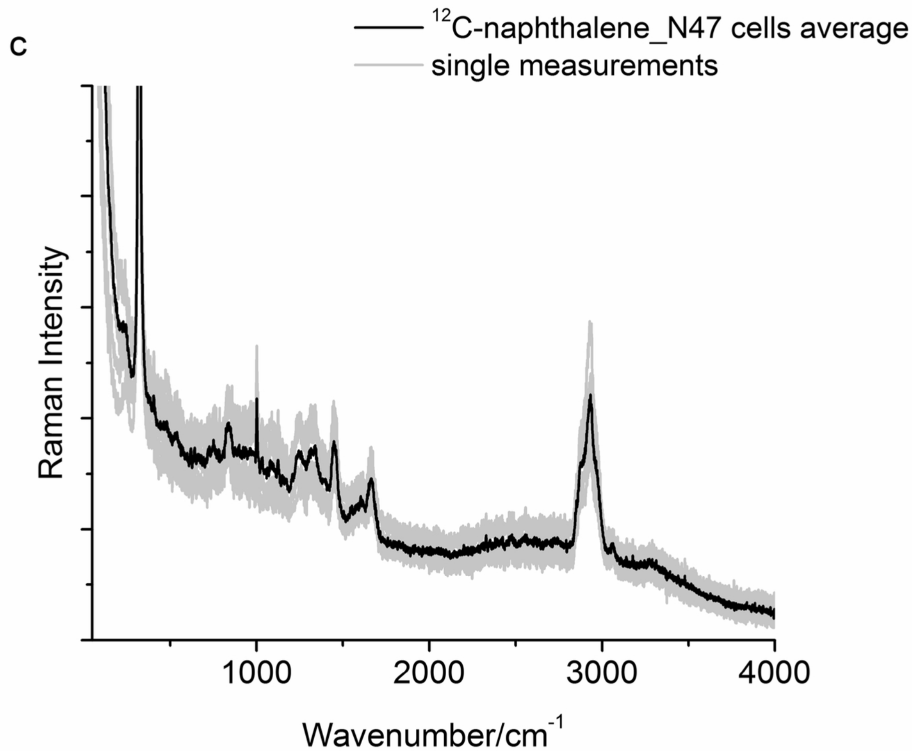

Figure 1 c
62x48mm (600 x 600 DPI)

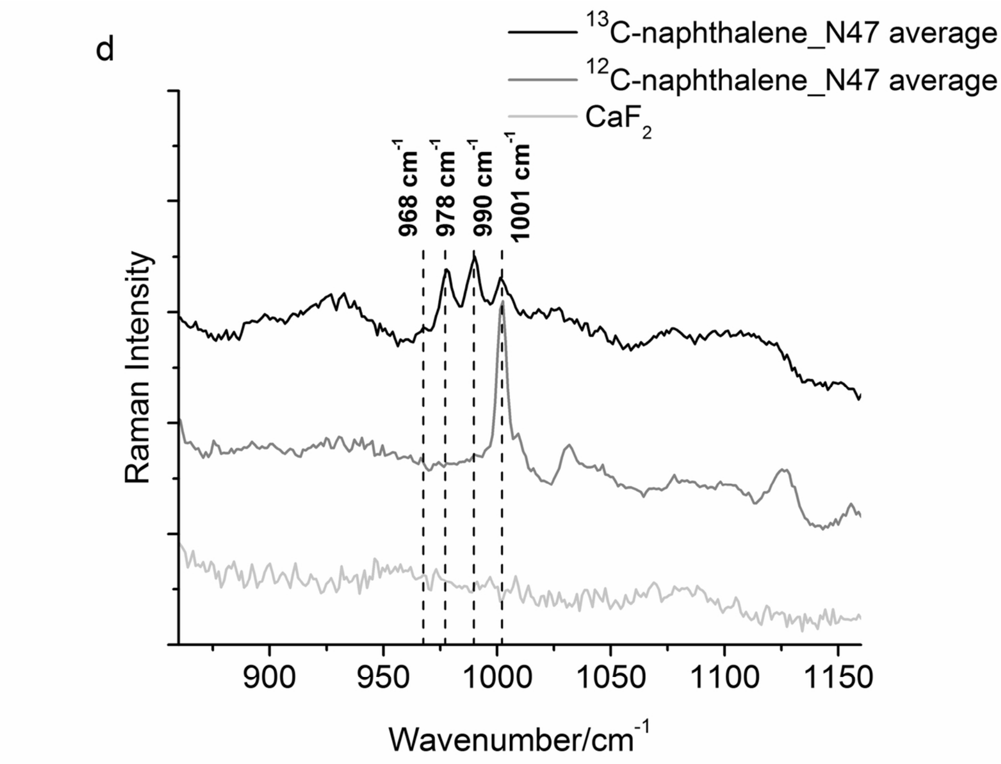

Figure 1 d
62x48mm (600 x 600 DPI)

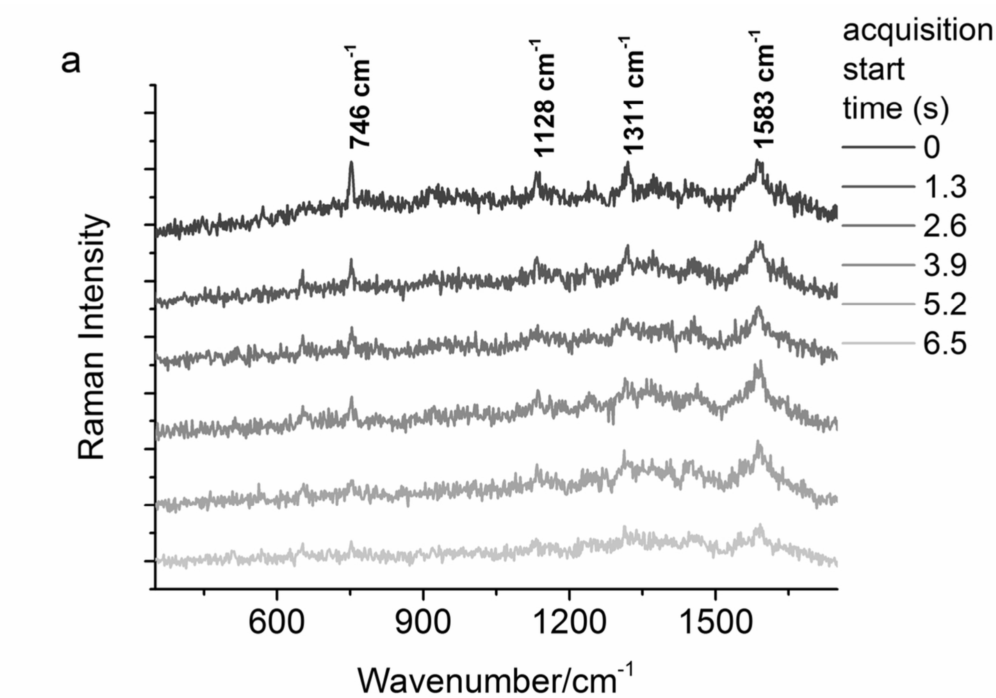

Figure 2 a
57x40mm (600 x 600 DPI)

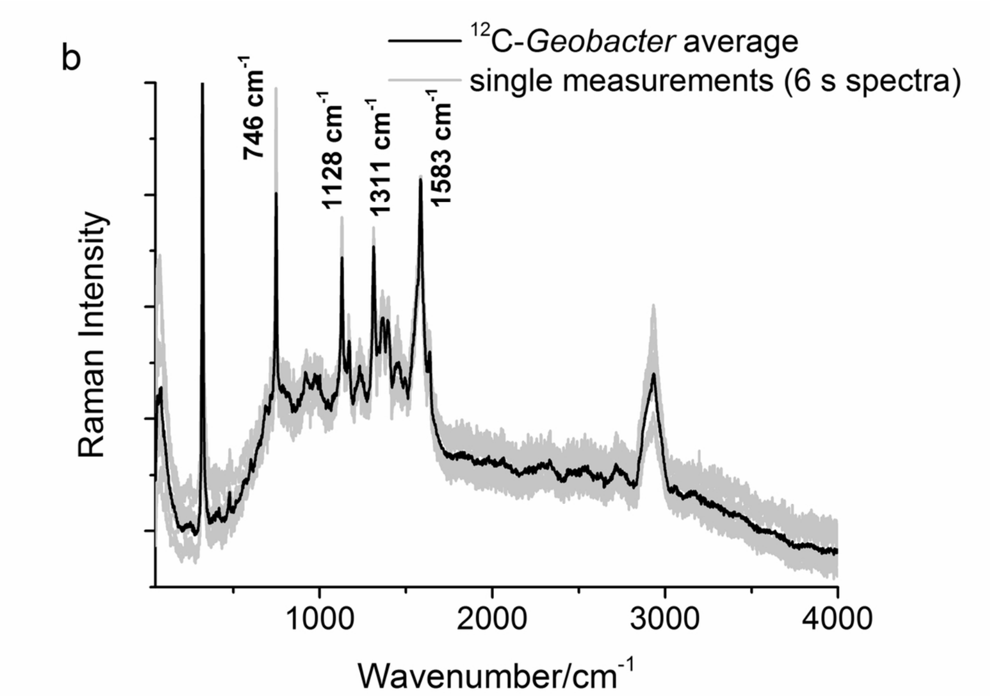

Figure 2 b
57x40mm (600 x 600 DPI)

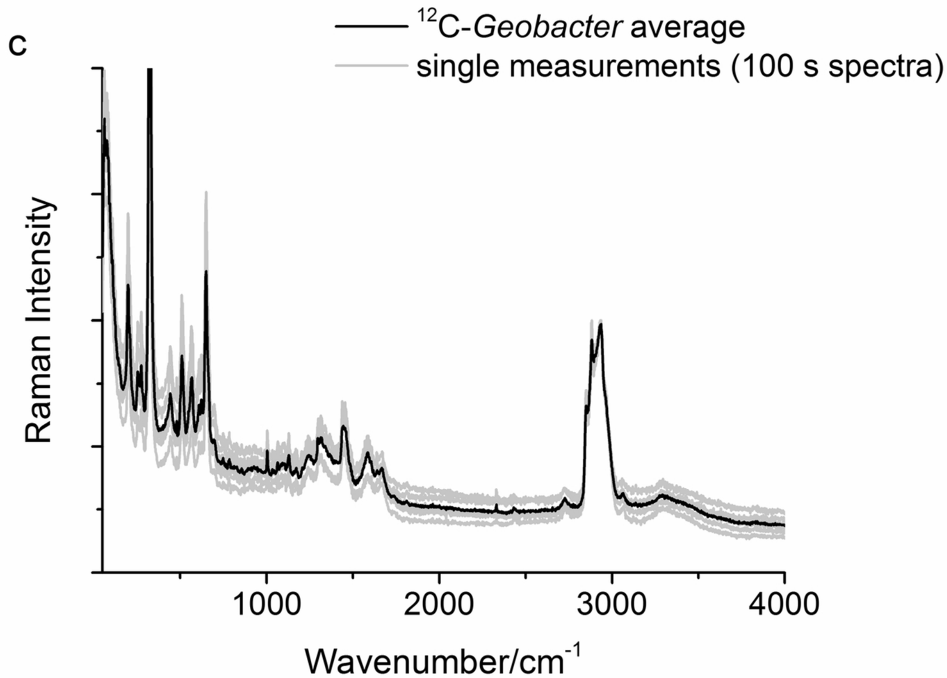

Figure 2 c
57x40mm (600 x 600 DPI)

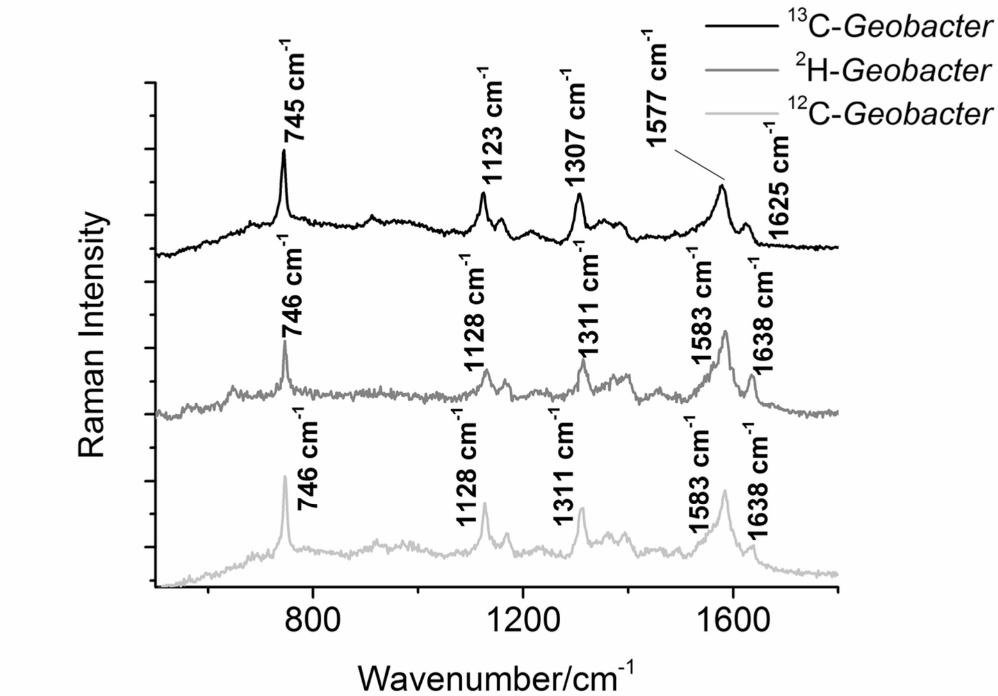

Figure 3
57x40mm (600 x 600 DPI)

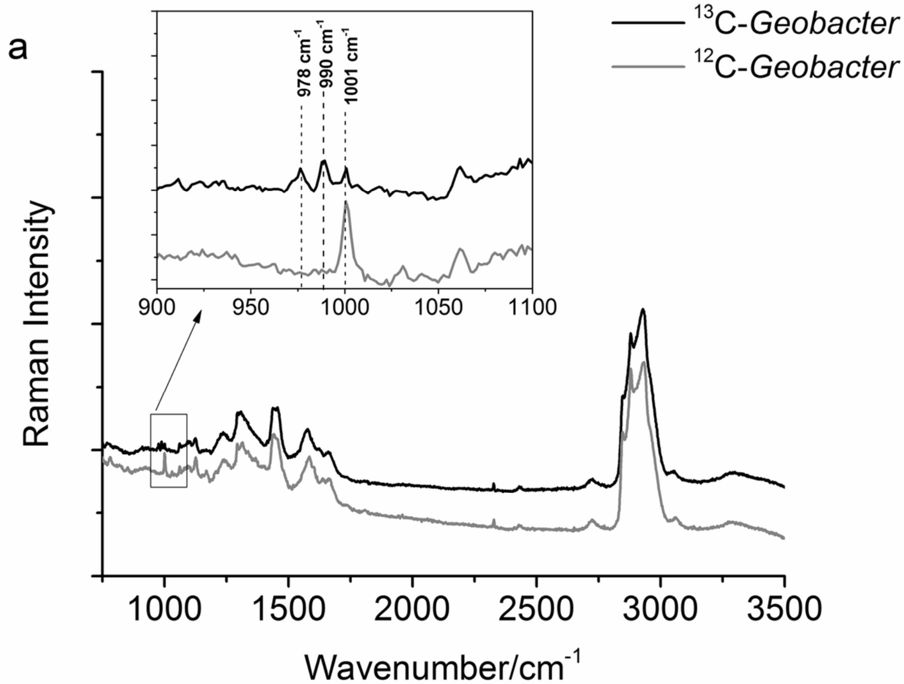

Figure 4 a
57x40mm (600 x 600 DPI)

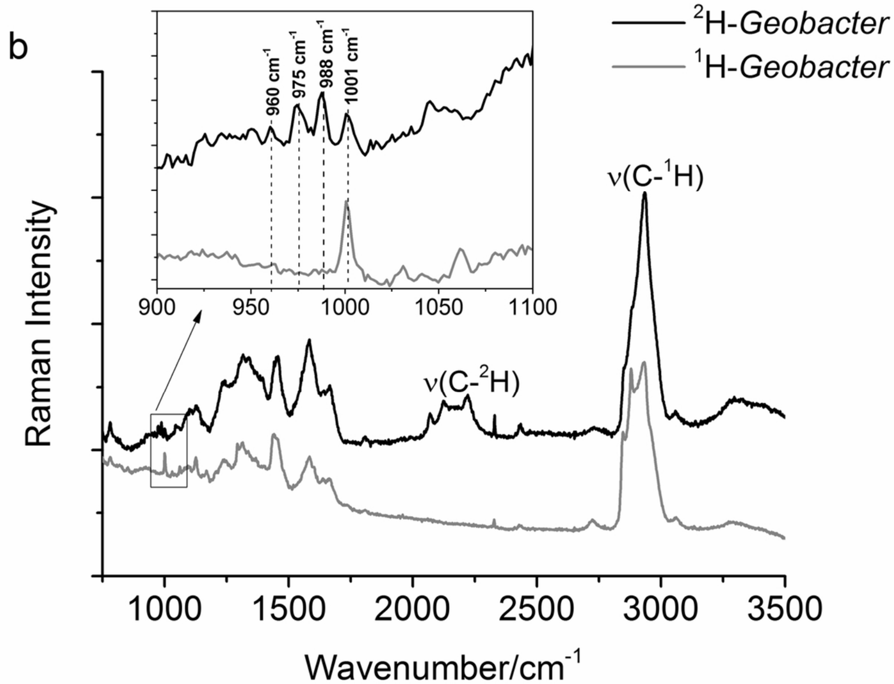

Figure 4 b
57x40mm (600 x 600 DPI)

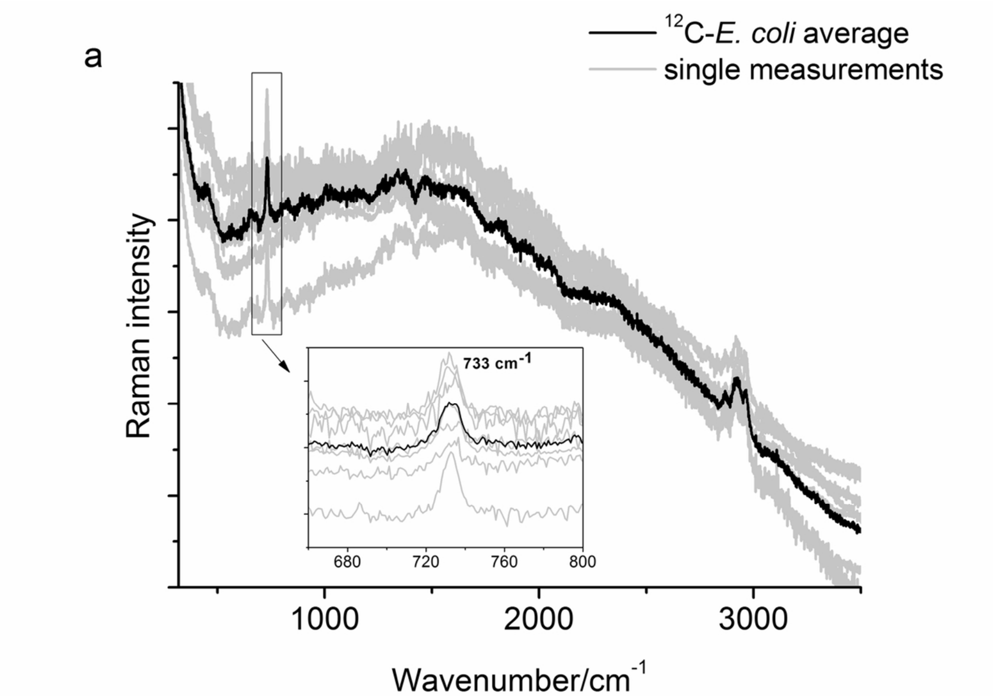

Figure 5 a
57x40mm (600 x 600 DPI)

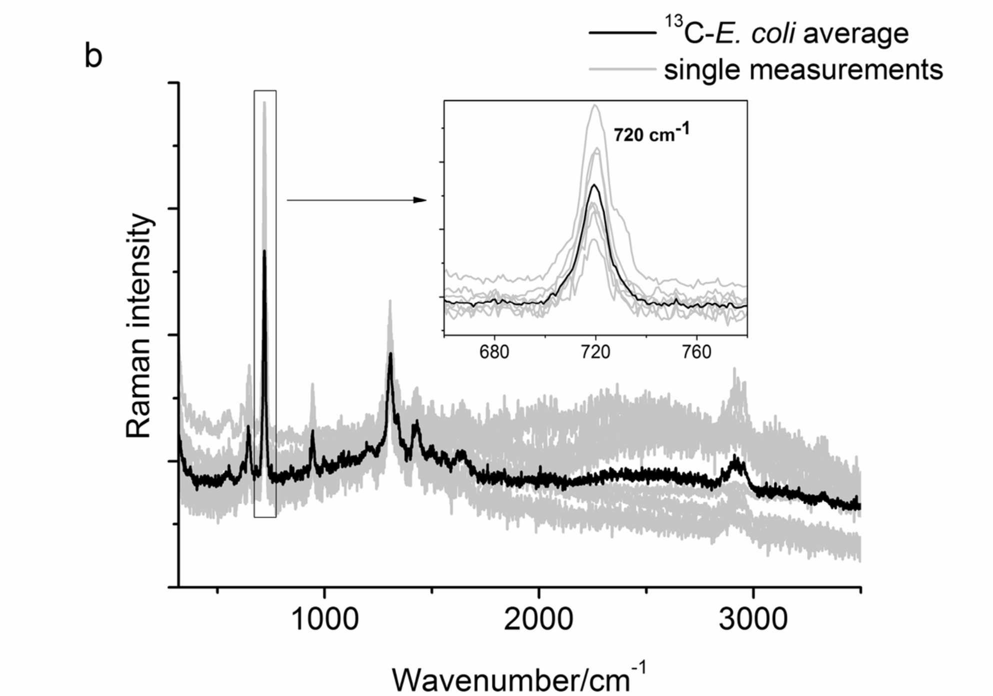

Figure 5 b
57x40mm (600 x 600 DPI)

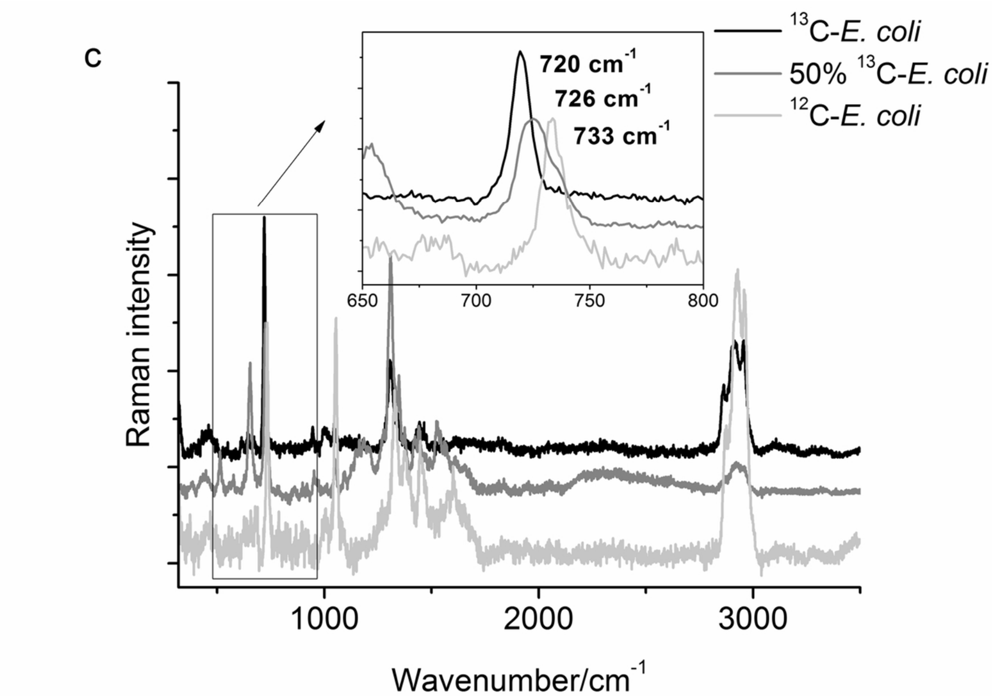

Figure 5 c
57x40mm (600 x 600 DPI)

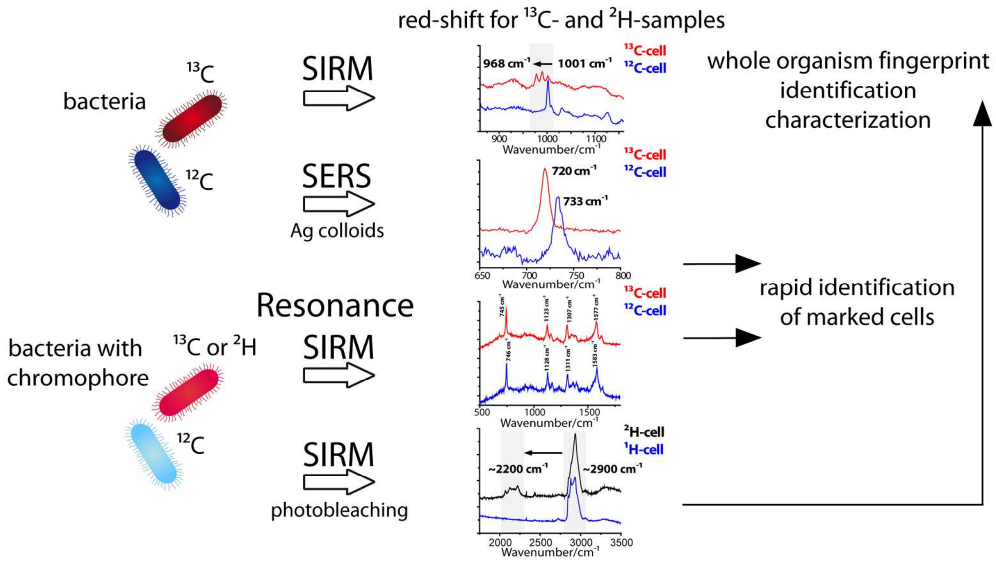

Figure 6
171x98mm (300 x 300 DPI)

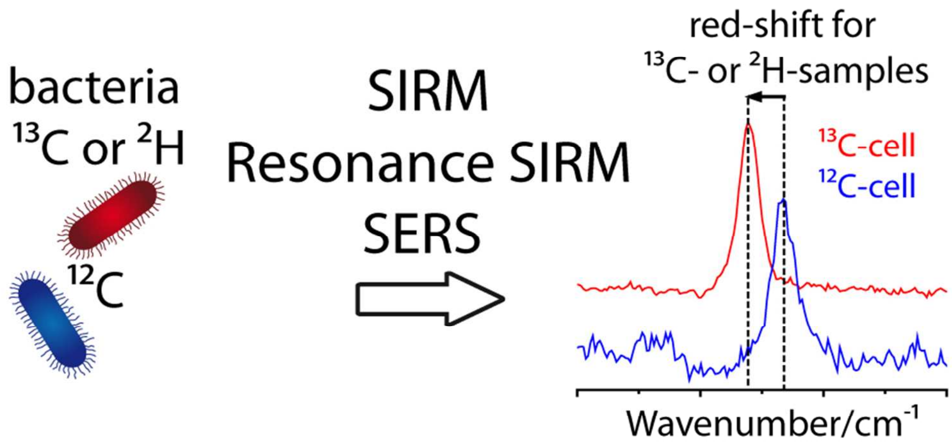

TOC
82x44mm (300 x 300 DPI)